Geophysical assessment of vulnerability of surficial aquifer in the oil producing localities and riverine areas in the coastal region of Akwa Ibom state, southern Nigeria

N. J. George[1], J. G. Atat[2], I. E. Udoinyang[3], A. E. Akpan[4] and A. M. George[4]

[1]Department of Physics, Geophysics Group, Akwa Ibom State University, Ikot Akpaden 520102, Nigeria
[2]Department of Physics, University of Uyo, Uyo, Akwa Ibom State 520101, Nigeria
[3]Rhema University Aba, Abia State 440001, Nigeria
[4]Department of Applied Geophysics Programme, Department of Physics, University of Calabar, Calabar 540222, Nigeria

1D resistivity sounding survey was combined with geological and geohydrochemical information in order to examine the aquifer vulnerability. Ten Schlumberger soundings were executed along one profile on the basis of proximity to functional boreholes. Ten samples of groundwater from nearby boreholes were checked for concentrations of significant trace element in the laboratory. The resistivity and geohydrochemical information were employed to examine the level of protection and the associated possible risk of the groundwater repository in the mapped area. The interpreted overburden parameters (resistivities and thicknesses) of water repositories were deployed to determine the integrated electrical conductivities (IEC) and susceptibility of hydrogeological units to surface contaminations. Based on results, Eket and Onna on the southern part of Nsit Ubium have IEC which reflect medium to poor protection capacity based on slightly protected and vulnerable protective layers above the underlain groundwater within the approximate depth range of 15–30 m. Nsit Ubium, the northern zone of the survey area, has a wide range of resistivity which creates windows or vulnerable pathways for percolation of waste pollutants from the surface which flow at the deeper layer. However, layers within 15–25 m depth provide good protection to their underlying aquifer based on IEC which are >1 Ω^{-1}. Hydrochemical parameters also show higher values that are beyond the 2006 World Health Organization (WHO) standards. The integration of resistivity data and the hydrochemical data showed that the dominant topmost cover layers of the study areas are grossly vulnerable due to drainable pores in the formation.

Keywords: Aquifer vulnerability, groundwater protective layer and IEC.

THE effectiveness of groundwater protection is supported by availability of layers characterized by highly significant thickness and low coefficient of permeability. This leads to high residence time of water percolation[1,2]. Based on this, protective layers that determine the protective capabilities of aquifers are known as homogenous layers. These bodies have coefficient of permeability and porosity as bulk properties[3]. Intrusion of sands or cracks in clay can cause non-homogeneities, which determine the pathways for percolation. The location of these pathways is known to be a unique problem to be assessed for a detailed vulnerability study[4].

Aquifer vulnerability is viewed as the sensitivity of the quality of underground water to contaminant load, determined by the essential properties of aquifer[5]. Pollution risk occasioned by vulnerability as well as the existence of pollutants entering the subsurface can be differentiated from this. According to Younger[6], aquifer vulnerability is the readiness of an aquifer to be polluted. It is defined by the characteristics of cover layer overlying the aquifer. In the study area, clay cap can act as protective layer, protecting the underlying Quaternary hydrogeological units. Interestingly, availability of sand or argillaceous lenses can be potential sites for vulnerability of hydrogeological units and this relates to texture of the inhomogeneous cap of argillite in which the existence of sand or silt lenses provides pathways for vulnerable zones or windows for contaminants to percolate into the aquifer[7].

Maps of saturated/unsaturated geological units can show the spatial spread of partially or wholly safeguarded layers for strategic pollution management. To decipher the degree of protection and the vulnerability of aquifers in the study area, the vertical electrical sounding (VES) survey was employed for identification of contamination susceptible lithology and protective layers through use of longitudinal unit conductance S and transverse resistance T, known as Dar-Zarrouk parameters[8].

Generally, confined aquifers with sizeable protective layers are usually not vulnerable to contaminant fluid load[9]. However, the unconfined or open aquifers are highly vulnerable to fluid contaminant load that percolates into

*For correspondence. (e-mail: nyaknojimmyg@gmail.com)

them. VES is a universal geophysical technique, that can lead to determination of the above hydraulic properties. In the distribution map of the transverse unit resistance of open hydrogeological unit, higher values are associated with zones corresponding to elevated transmissivity. These zones can therefore be classified as regions prone to contaminations due to high permeability and hence monitoring can be recommended for checking of contamination. Longitudinal conductance can be used to characterize the permeability or transmissibility confining argillaceous layers. The spread of longitudinal conductance (per Ω) can be greater or less than unity. Theoretically, when $S > 1.0$ Siemens, the interpretation suggests efficient protection by the layer and percolation of fluid contaminant load is substantially reduced, thereby making the aquifer protected[9]. However, when $S < 1.0$ Siemens, there is high risk of contamination as the zones are susceptible to contaminant fluid percolation due to high permeability of the drainable layers[10].

Description of the study area

The study area is situated between 4°30′–4°50′N and 7°30′–8°15′E as given in Figure 1. In terms of geology, the survey area cuts across the Calabar Flank and Sedimentary Basins of Niger Delta[11]. About 80% of the Niger Delta area is made up of Akata, Agbada and the Benin formations in ascending order. Groundwater is tapped from the top of statigraphic sequence[12]. Imo Shale and Benin formations are shallowly exposed in the survey area[13]. The geological succession in the study area in Table 1 indicates the transition of arcuate delta into Atlantic Ocean. This succession represents transgression and regression that characterized the growth of the sedimentary basin in the southern part of Nigeria[14]. The Bende–Ameki Group indicates the continued regressive phase. The survey area falls into the low-lying Benin Formation in southern Nigeria[15,16]. The drainage in mapped area is made possible by the Kwa River, cross rivers and Etim Ekpo tributaries[17]. Studies conducted in the study area indicate that fine to gravelly sand within the depth range of 65–100 m serves as economic water repository[16–19]. The saltwater-freshwater incursion in the area takes place below the aquifer cover layer considered in this study[16]. Vegetation in the study area is tropical rainforest type[18]. The noticeable wet and dry seasons are characterized by unstable amount of precipitation (230 to 390 mm monthly) and variation of temperature[19]. Table 1 gives the lithologic and stratigraphic correlation of hydrogeologic units of the study area. The delineated units are the upper, middle and lower sand hydrogeological units, arranged in increasing order of geologic age and depth of burial. The broadest hydrogeological unit is middle aquifer, which abuts on the lower sand aquifer by aquitard of Imo shale. The discussions of these units are chronologically taken in order using boreholes[13,16].

This study aims at investigating the protective or covering layer of shallow aquifers for detailed information concerning the protection, susceptibility and vulnerability of aquifers in the survey area.

Method and data acquisition

Ground-based resistivity measurements for data acquisition were carried out in the study area. Ten VES were carried at stations whose coordinates were established with global positioning system (GPS) along a profile in three local government areas. The Schlumberger array with two pairs of electrodes, a pair for energizing current and a pair for measuring potential generated, was employed with maximum current-electrode (AB) of 600 m to 800 m depending on accessibility. SAS 4000 ABEM terrameter was the equipment used. VES technique was chosen because of the speed and versatility associated with field operations and less operational difficulties[20].

Application of Dar-Zarrouk parameters

Theoretically, resistivity and thickness of stratified geological materials can be conceptually studied using longitudinal unit conductance (S) and transverse unit resistance (T) using the Dar-Zarrouk (Dz) parameter expressed in eqs (1) and (2) for n-horizontal, homogenous and isotropic layers of resistivity ρ_i and thickness h_i (refs 21, 22)

$$S = \sum_{i=1}^{n} \frac{h_i}{\rho_i}, \tag{1}$$

$$T = \sum_{i=1}^{n} \rho_i h_i. \tag{2}$$

Layer resistivity is applied for estimating the degree of protection of vadose zones as the protective strength of argillaceous overburden covering arenaceous sub-surface is directly related to its longitudinal unit conductance S that has the dimension of time known as infiltration time[10]. The environmental impact directly affects groundwater vulnerability through the surface environmental processes that pollute the subsurface water on global scale[23]. Many methods, which depend on hydrogeologic setting are abound for vulnerability assessment. However, the aquifer index of vulnerability is predominantly utilized to examine the susceptibility and vulnerability of groundwater contamination to surface flow[23]. The vulnerability index links the hydraulic resistance C, of unsaturated cap unit to vertical flow of contaminated water through eq. (3)

$$C = \sum_{i=1}^{n} \frac{h_i}{k_i}, \tag{3}$$

where k_i and h_i are, coefficient of permeability and thickness respectively of the aquifer overburden. For sandy

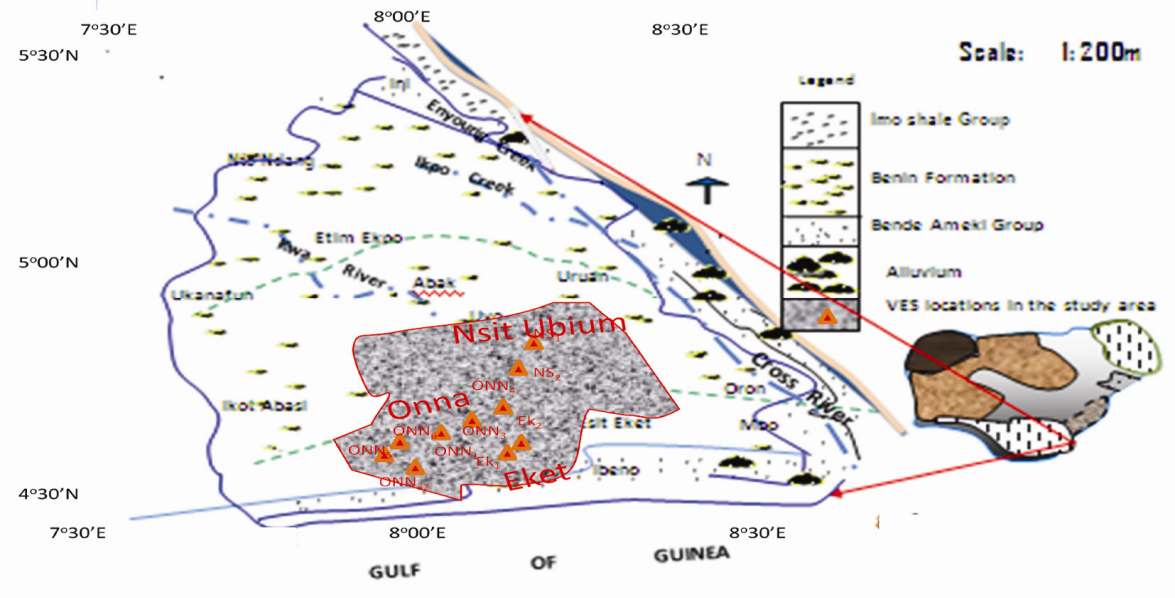

Figure 1. Location and geology map of the study area showing the VES points.

Table 1. Stratigraphic and hydrostratigraphic units in Akwa Ibom State, Nigeria (after ref. 13)

Age		Group/Formation	Lithology	Aquifer
Quaternary	Recent	Alluvium ridges	Gravel, lateritic sand, fine to medium grained sand and carbonaceous sand Unconsolidated sand and gravelly sand with clayed intercalations	Upper sand
	Pliocene Pleistocene	Benin Formation/ coastal plain sand		
Tertiary	Oligocene Miocene	Ogwashi Asaba	Grit and sand with intercalations of clay and lignite seams Semi consolidated sandstone plus minor shale	Middle
	Middle Eocene	Benede–Ameki group		
	Paleocene Early Eocene	Imo shale group	Shale with thinner sandstone and band of fossiliferous limestone	Aquitard
Cretaceous	Maastrichtian	Nauka Formation and Ajali sandtstones	Lateritic sandstone and minor shale	Lower sand

materials, k values range from 10^{-5} to 10^{-1} m/s. These values are of higher order, greater than those of argillite-dominated layers. The C values are predetermined by aquifer depth and the hydrogeological formation above it[24]. Locally, hydraulic resistance is employed as coarse estimate of the vertical time of travel of water in the overburdened unsaturated formation. The vertical time of travel of water in the top unsaturated formation can be linked to the geologically dependent conductivity properties or its converse, resistivity[25].

Effective porosity or permeability predicts the hydraulic resistance of argillaceous and arenaceous materials. In view of this, hydraulic resistance and effective porosity determine the electrical conductivity or resistivity of geological materials[3]. Therefore, hydraulic conductivity can be replaced either by resistivity ρ_i or conductivity σ_i to estimate (C) known as integrated electrical conductivity (IEC)[25], or a geophysical based index of protection[1]. The vulnerability of aquifer can be assessed through IEC expressed in eqs (4) and (5)

$$\text{IEC} = \sum_{i=1}^{n} h_i \cdot \sigma_i, \tag{4}$$

or

$$\text{IEC} = \sum_{i=1}^{n} \frac{h_i}{\rho_i}, \tag{5}$$

where $\sigma_i = 1/\rho_i$.

The resistivity (ρ_i) and thickness (h_i) for the above aquifer layers can be estimated through 1D or 2D geoelectric measurements. As seen in IEC expression, higher values of IEC can be realized when the overburden

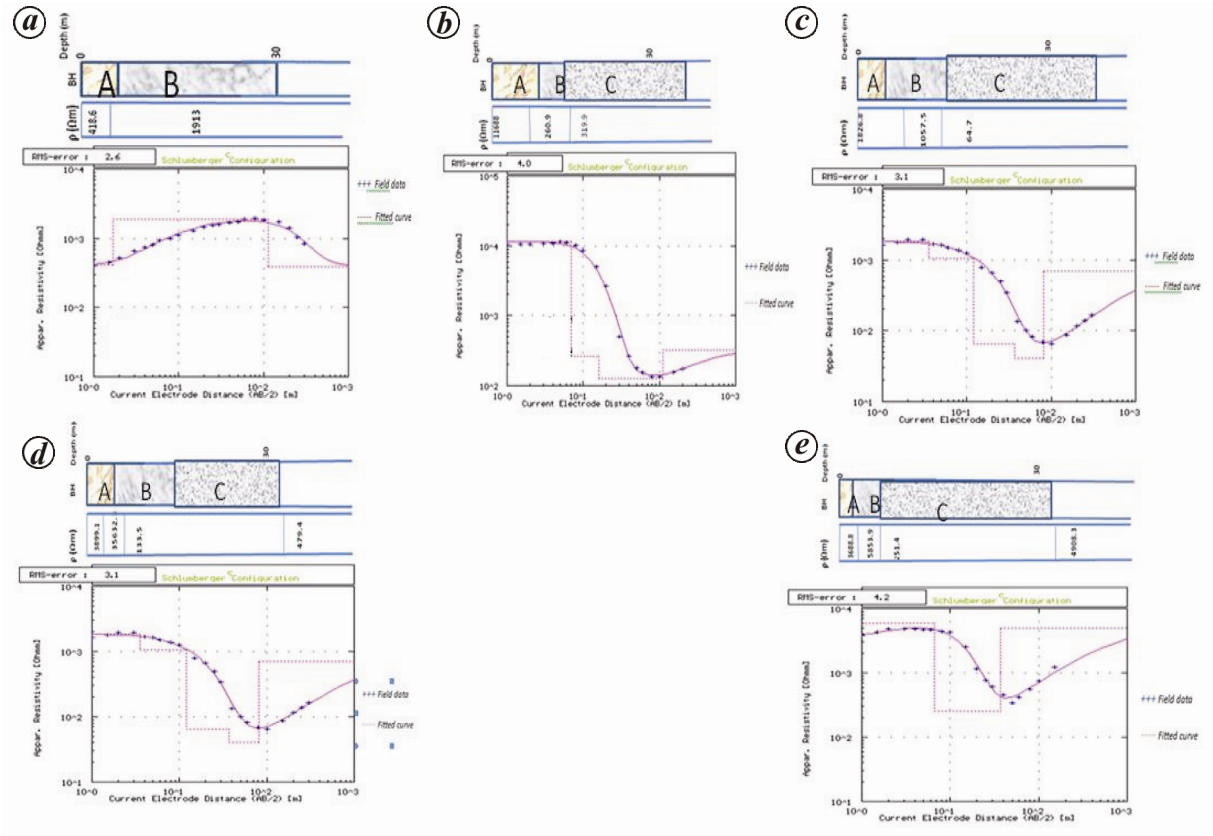

Figure 2. ***a***, Correlation between the interpreted resistivity of shallow layers model in Eket (Ek_1) and lithology data from the nearby borehole (A, inhomogeneous gravelly sand mixed with river sand and minor sandy clay; B: Fine-medium grained sands); ***b***, Correlation between the interpreted resistivity of shallow layers model in Eket (Ek_2) and lithology data from the nearby borehole (A, inhomogeneous gravelly sand mixed with river sand and minor sandy clay; B: Fine-medium grained sands; C, Fine sands mixed with minor clay at regular interval); ***c***, Correlation between the interpreted resistivity of shallow layers model in Nsit Ubium (NS_3) and lithology data from borehole (A, inhomogeneous gravelly sand mixed with river sand and minor sandy clay; B, Fine-medium grained sands; C, Fine sands mixed with minor clay at regular interval); ***d***, Correlation between the interpreted resistivity of shallow layers model in Onna (ONN_5) and lithology data from the nearby borehole (A, inhomogeneous gravelly sand mixed with river sand and minor sandy clay; B, Fine-medium grained sands; C, Fine sands mixed with minor clay at regular interval) and ***e***, Correlation between the interpreted resistivity of shallow layers model in Onna (ONN_7) and lithology data from the nearby borehole (A, inhomogeneous gravelly sand mixed with river sand and minor sandy clay; B, Fine-medium grained sands; C, Fine sands mixed with minor clay at regular interval).

layer has reasonable higher thickness and lower resistivity. This condition will give rise to good protection to groundwater against surface contaminant load[1].

Results and discussion

The curve samples in Figures 2–6 were chosen due to their proximity to borehole lithologic logs. Hydrological and hydrochemical data indicate that the top layers within the area considered for vulnerability and protection studies are inhomogeneous, porous and permeable. Since aquifer vulnerability and protection are considered in this paper, the representative curves were presented along with the drilled well lithology to evaluate the degree of protection within the protective layer which is considered to lie between 2 and 30 m depth as indicated in Figure 2 *a–e*. The values of the resistivities realized in the topmost layer (0.6–7.0 m) are extremely high (148–1168 Ωm) with average value of 3282 Ωm (Table 2). The high variation in resistivity values for the topmost layer agrees with the description of the layer as resistive inhomogeneous layer that has grain size of gravelly sand intercalated with argillaceous materials according to borehole lithologs. The second layer according to geoelectric soundings, constrained by geological description, shows high value of resistivities with an average of 8144 Ωm. The high average resistivity indicates that the second layer is the extended transition of the topmost layer which is a combination of the river sands, fine to medium grained sand and clayey sand in irregular proportion. The third layer shows a great inversion of resistivity with depth, as range and average are 43–3711 Ωm and 500 Ω respectively. This layer is in agreement with the lithologs near the representative soundings in Figure 2 *a–e* and is described as fine sands interlaced with clay at some locations. The models show inhomogeneous layers due to variation of sandy materials at depth that is

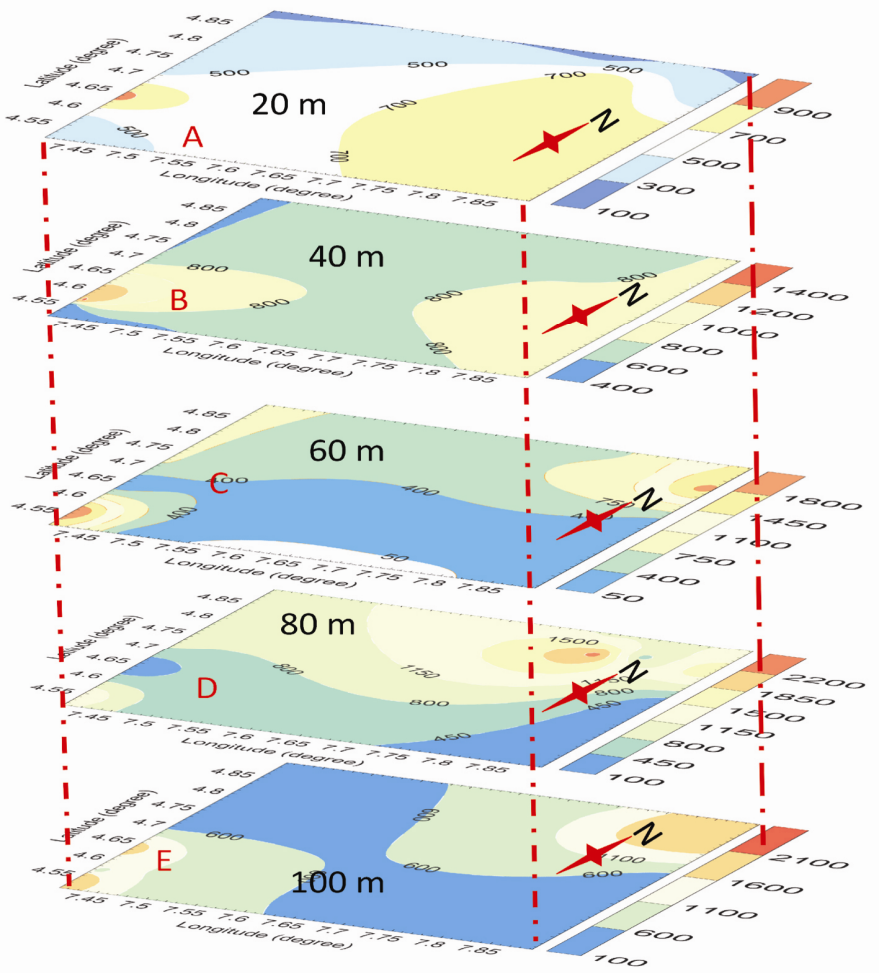

Figure 3. Apparent resistivity distribution maps A, B, C, D and E for 20 m, 40 m, 60 m, 80 m and 100 m half current electrode separations respectively from top to bottom.

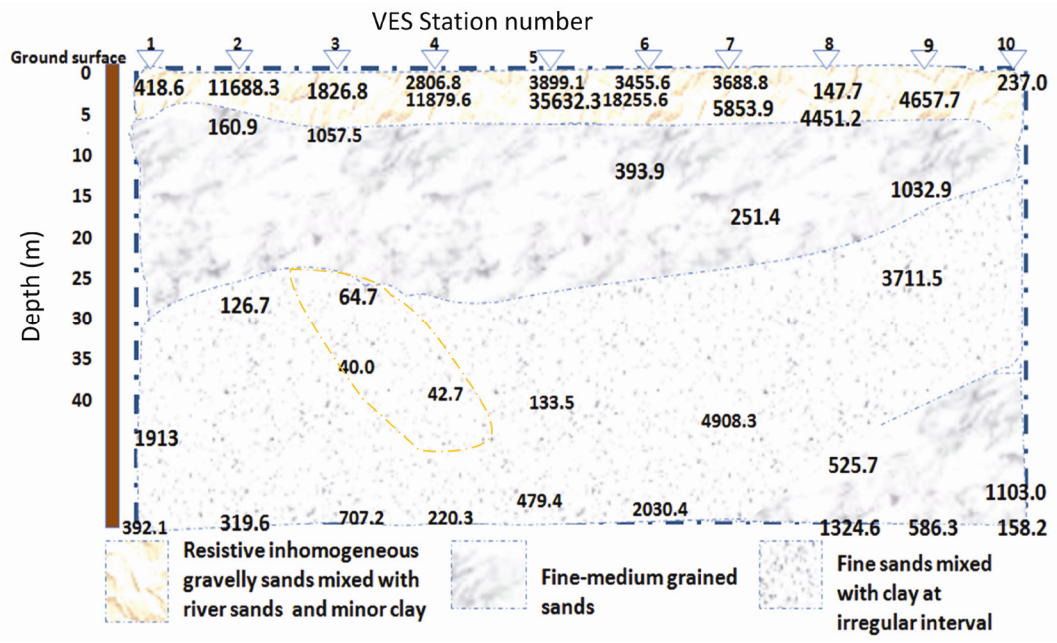

Figure 4. Geoelectric cross-section of the assessed protective layers of the aquifers (the dotted enclosed ring in layer three shows some regions of irregular argillites picked by current) in the area.

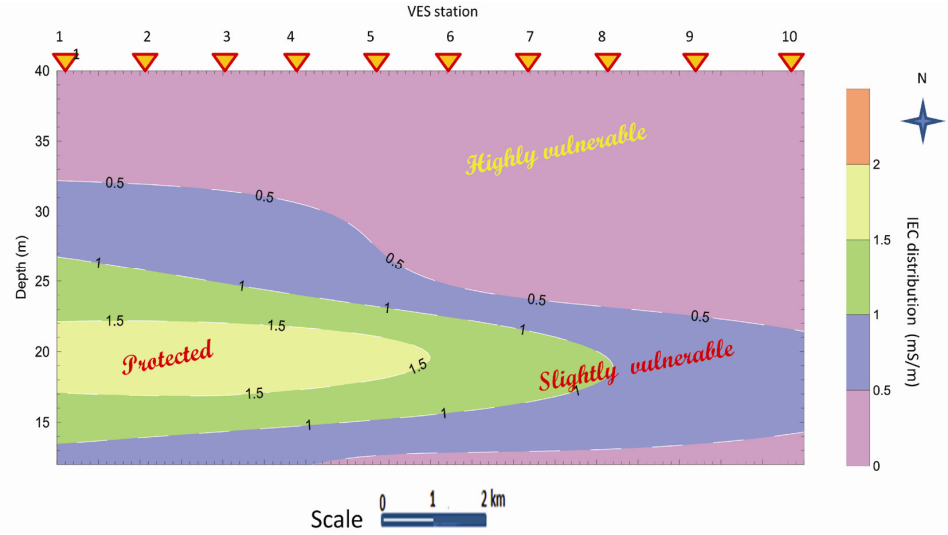

Figure 5. Distribution of IEC along the assumed protective layers of the underlain aquifers.

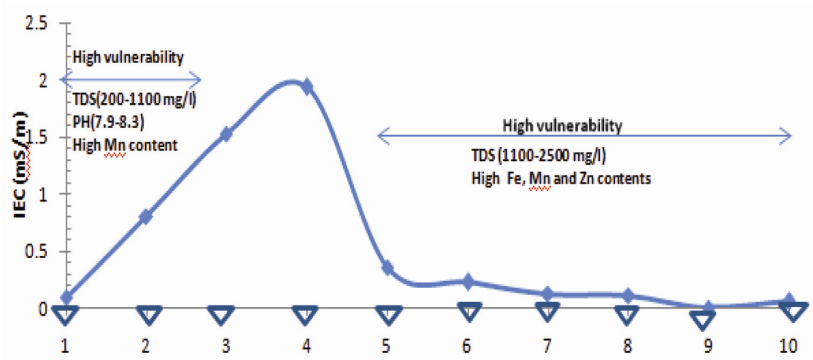

Figure 6. Estimated profile of IEC from Schlumberger soundings showing the region of high vulnerability.

considered to be the protective layer of the underlying aquifers. These models also show the level of vulnerability of the top layers and their susceptibilities to infiltration of contaminant fluids from the surface flow due to their inhomogeneities. The apparent resistivity maps for half current electrode separations ($AB/2$) for 20, 40, 60, 80, and 100 m for A, B, C, D and E respectively are shown in Figure 3. The topmost layer A shows apparent resistivity distribution that varies with B. 'A' and 'B' in the figure can be roughly viewed to have sampled the apparent resistivity within the depth of about 7 and 13 m respectively, since half of the current electrodes is one third of real depth of current penetration[22]. The variation observed between $AB/2 = 20$ m and $AB/2 = 40$ m in *A* and *B* respectively is an indication of inhomogenity of the sandy formation that causes variation in resistivity values and geohydraulic properties of the unsaturated protective layer. At $AB/2 = 60$ m (about 20 m deep), the apparent resistivity map also shows a great variability from the top layers[26]. However, in *D* and *E* half current electrode separation value of 80 m and 100 m, reflection on the maps gives respective depths of 27 m and 33 m. Due to the inhomogeneous nature of the upper protective layers, the open aquifers within the depth of 30 m to 50 m are highly vulnerable and unprotected (Figure 4). The drainable geoelectric layers in Figure 4 display the resistive inhomogeneous gravelly sands mixed with river sands and minor argillites on top within a depth range of about 0–5 m depth. The second layer (about 5–30 m) and third layer (>30 m) respectively display drainable fine–medium grained sand and fine sands erratically interlaced with minor argillites at certain locations. These cover layers have high porosity[27] and as such serve as pathway/window for infiltration of the surface flow into the economic aquifers located within depth range of 65–100 m. From the lithologs, there are no clear-cut layers of protection within 30 m depth. However, the description of the lithology emphasizes on minor intercalations of clay (the protective materials) with sandy formation. On the basis of the characteristics of the covering layers, the aquifer is highly vulnerable and unprotected.

Since vulnerability of groundwater implies susceptibility of groundwater to contamination, it can be inferred that groundwater susceptibility to contamination depends

Table 2. Interpreted resistivity result of the measured sounding points

VES no.	Location	Resistivity (Ωm)					Thickness (m)				IEC (mS/m)
		ρ_1	ρ_2	ρ_3	ρ_4	ρ_5	h_1	h_2	h_3	h_4	
1	Eket	418.6	1913	392.1	–	–	1.7	112.3	–	–	0.100
2	Eket	11688.3	260.9	126.7	319.6	–	7.0	8.9	94.5	–	0.800
3	Nsit Ubium	1826.8	1057.5	64.7	40.0	7072	3.2	8.5	24.6	45.2	1.523
4	Nsit Ubium	2806.8	11879.6	42.7	220.3	–	0.6	3.8	82.7	–	1.937
5	Onna	3899.1	35632.3	133.5	479.4	3529.8	1.0	2.9	30.9	27.6	0.358
6	Onna	3455.6	18255.6	393.9	2030.4	–	0.6	2.0	89.2	–	0.226
7	Onna	3688.8	3853.9	251.4	4908.3	–	0.8	5.7	30.6	–	0.122
8	Onna	147.7	4451.7	525.7	1324.6	–	0.5	5.6	54.7	–	0.110
9	Onna	465.7	1032.9	3711.5	586.3	–	2.6	7.9	23.4	–	0.005
10	Onna	237.0	1103.0	158.2	–	–	0.6	59.4	–	–	0.056

on site characteristics. Hence, in different formations of hydrogeological conditions differing vulnerabilities and degrees of protection are expected. Since vulnerability is a characteristic that is independent of the nature of pollutant, it is necessary to consider the spatial distribution of controlling properties that were geophysically determined.

The development of geoelectric cross-section in Figure 4 based on resistivity and depth information (Table 2) spatially shows that, what is considered to be the protective layers of the unconfined aquifers are generally drainable and permeable. These layers provide windows for contamination of the underlying aquifer that seemed to be naturally open to infiltration and contaminations from the surface and near surface flows. However, using a geophysically based protection index or IEC in Figure 5, the vulnerability of the underlying aquifers was discerned. Figure 5 shows distribution of IEC in (ms/m) with depth. Being a topographically low area, the watertable seems to be near to surface and the IEC values vary between 0.005 (ms/m) in Onna and 1.937 (ms/m) at Nsit Ubium. The IEC distribution map indicates that the protective layers at Nsit Ubium have IEC values greater than 1 Ω^{-1} while that of the adjoining Eket and Onna are grossly less than or equal to 1 Ω^{-1} in most places sampled. The map shows on the average, vulnerable, slightly vulnerable and protected layers respectively from water samples obtained at various depths of protection of drilled holes within the considered protective layer.

Figure 6 shows the estimated IEC distribution from Schlumberger sounding for the ten soundings that were made on the basis of proximity to borehole in the study area. It also shows the physical and chemical properties which were measured from water samples collected from boreholes. Nsit Ubium, sandwiched between Eket in the southwest and Onna in the southeast, has an estimated IEC greater than 1 Ω^{-1} (VES 3 and 4) while that of Eket and Onna lie below 1 Ω^{-1} (VES 1, 2, 5, 6, 7, 8, 9 and 10). Besides, Eket and Onna (oil cities) seemed to have high contents of Fe, Mn and Zn beyond the 2006 WHO standards for potable water shown in Table 3 (ref. 27). These areas have very high vulnerability which is proved by the observed properties to be natural due to the drainable pores of overlying formation covering the aquifers and artificial due to oil spills which kill the iron bacteria (Leptothrix, Clonothrix and Gallionella) that provide clogging effects to formations that are susceptible to contamination. The total dissolved solids were found to be 200–2200 mg/l in Eket while in Onna water samples, the range was 1103–2500 mg/l. The values were all found to be beyond the 2006 WHO standards (500 mg/l) for potable water and this also contributes to their artificial vulnerability. The contamination of groundwater in these regions is also viewed to be due to salt water intrusion in marine water bodies that surround Eket and Onna local government areas. Although the geochemical data indicate elevation beyond the WHO standard for drinking water, indicating the possibility of saltwater–freshwater incursion within the layers below the protective cover in the region, the topographically low coastal zone is characterized by vadose zones that are drainable and susceptible to anthropogeically polluted matter based on longitudinal conductance that is less than 1 Siemens[16,19].

The IEC in Figure 6 shows that the gravity of protection in the oil cities is low on an average, with inhomogeneous protective layers that have windows for surface waste infiltration into the phreatic zones. The water samples near VES 1 and 2 in Eket have high groundwater pollution characterized by anomalously high pH value (7.9–8.3), which is associated with total dissolved solids. The high vulnerability in the area is related to the total silt and fine sand lenses in the inhomogeneous protective layers. The resistivity values of some of the sizably thick layers within the depth of 20–30 m deep suggest of aquifers that are likely to bear clean water in the middle zone (Nsit Ubium); however, the high salinity intrusion within the adjoining boundaries of Eket and Onna and the infiltration through the aquifer covering layers substantially reduce the protection index in the area.

In the area where salt water intrusions are major causes of vulnerability, sandy formation saturated with salt

Table 3. Concentration of trace elements of water samples

VES no.	Location	Depth (m)	Water sample	pH	TDS (mg/l)	Trace elements (Mg/l)		
						Fe	Zn	Mn
1	Eket	35	1	7.9	1100	0.53	3.2	0.62
2	Eket	30	2	8.3	200	0.11	3.5	0.51
3	Nsit Ubium	17	3	7.2	300	0.24	<3.0	0.31
4	Nsit Ubium	20	4	7.4	240	0.27	<2.5	0.29
5	Onna	12	5	9.00	1200	0.50	3.2	0.45
6	Onna	32	6	9.31	1100	0.63	3.7	0.48
7	Onna	25	7	7.81	2400	0.81	3.2	0.51
8	Onna	35	8	7.7	2450	0.92	3.9	0.41
9	Onna	36	9	8.6	2500	0.73	3.1	0.63
10	Onna	40	10	7.6	2300	0.67	3.0	0.42
WHO (2006)*				7.5	500	0.30	0.4	3.0

*Acceptable WHO standards of parameters[27].

water may indicate extremely low value of resistivity when compared to what the upper clay cap for a functional protective zone can show. It is impracticable to differentiate saltwater sands from argillite-dominated conductive fluid from VES measurements without borehole constrained information. Therefore, the estimate of longitudinal unit conductance is a function of accuracy in the VES data interpretation. It is almost impossible to estimate the pollution extent of distribution in a site to a satisfying degree without borehole inputs. Since the earth naturally filters fluid seepage, its capacity to decelerate and trickle percolating fluids depends on its protective capacity[18]. Based on this, it is important to note that higher the transmissivity–transverse resistance ratio, the better is the protection. With highly resistive vadose zone, indicating very low transmissivity-transverse resistance ratio, the phreatic zones are highly susceptible to contaminants from vadose zone in addition to saltwater–freshwater incursion within the phreatic zones.

Conclusion

This study aims at applying 1D resistivity interpretation technique, together with hydrogeological and hydrochemical parameters for examination of vulnerability and susceptibility of aquifer to near surface and surface contaminations. The study site was located near boreholes in the oil producing cities of Niger Delta, Nigeria due to existing doubt regarding the vulnerability of aquifer. The interpreted primary data of thicknesses and resistivity were employed to gauge the index of vulnerability of overburdened layers in the Quaternary aquifer[28]. The results obtained from integration of the Schlumberger sounding, constrained by the nearby borehole and hydrochemical parameters of shallow lithology, provide a graphic detail of lithology of aquifer overburden materials that control the percolation of contaminant flow within the study area. The saltwater–freshwater incursion takes place within the phreatic zones, below the considered drainable vadose zone[19]. The resistivity distribution in the area gives an indication of inhomogeneous covering layer which overlies the phreatic zones. In many VES stations, the interpreted earth's models indicated significantly resistive bodies with recognizable anomalies within the vadose zone, indicating preferential pathway for waste pollutants from the surface flows. Alternatively, the arenaceous aquifer shows irregular drops of resistivities in some locations indicating saltwater–freshwater incursion within the phreatic zones. This represents another environmental problem in the area. In the study area incessant and excessive pumping of groundwater can negatively affect groundwater quality. This is possible because upward flow of saltwater or lateral and downward flow of waste water in the inhomogeneous covering layers may pollute groundwater in their repositories. In view of this, a sustainable pumping regulation and continuous regulated system of monitoring is needed for protection of open hydrogeological units tapped in the area. Index of protection, lithology of the protective layer and elevated TDS, Mn, Fe and Zn beyond that of 2006 WHO standards[29–31] presuppose that protection of aquifer is poor as aquifers are open to surface contamination through the covering layers and saltwater intrusion due to marine water bodies around the study area.

On the whole, mapping of vulnerability on the basis of resistivity data can give good information about protection and management of geohydro-resources. Vulnerability maps can be used to create healthy awareness about the potential risk associated with exposed hydrogeological units. Although vulnerability mapping is the relative vulnerability of the aquifer on the basis of available resistivity data associated with different levels of noise, quality control and resolution can be achieved with high degree of fidelity through the use of many data points and borehole constraint. This work serves as a baseline study in the study area for interpretation of vulnerability mapping involving integration of resistivity, geological and hydrogeological data and it may improve the accuracy in

an attempt to determine site specific vulnerability in an area.

1. Casas, M., Himi, Y., Diaz, Y. and Pinto, V., Assessing aquifer vulnerability to pollutants by electrical resistivity tomography at a nitrate vulnerable zone in NE Spain. *Environ. Geol.*, 2008, **54**, 515–520; doi:10.1007/s00254-007-0844-1.
2. Kirsch, R., *Groundwater Geophysics – A Tool for Hydrology*, Springer Berlin Heidelberg, 2006, pp. 454–471.
3. Kirsch, R., Sengpiel, K. P. and Voss, W., The use of electrical conductivity mapping in the definition of an aquifer vulnerability index. *Near Surf. Geophys.*, 2003, **1**(1), 13–19.
4. Foster, S. S. D., Fundamental concepts in aquifer vulnerability, pollution risk and protection strategy: In *TNO Committee on Hydrological Research, the Hague, Vulnerability of Soil and Groundwater Pollutants* (eds van Duijvenbooden, W. and van Waegeningh, H. G.), Proc. Inf., 1987, vol. 38, pp. 69–86.
5. Lobo-Ferrida, J. P., The European Union experience on groundwater vulnerability assessment and mapping. *COASTIN, A Coastal Policy Res. Newsl.*, 1999, **1**, 8–10.
6. Younger, P. L., *Groundwater Environment: An Introduction*, Blackwell Publishing, Oxford, UK, 2007, Ch. 9.
7. George, N. J., Akpan, A. E. and Ekanem, A. M., Assessment of textural variational pattern and electrical conduction of economic and accessible quaternary hydrolithofacies via geoelectric and laboratory methods in SE Nigeria: a case study of select locations in Akwa Ibom State. *J. Geol. Soc. India*, 2016, **88**, 517–528.
8. Obianwu, V. I., George, N. J. and Okiwelu, A. A., Preliminary geophysical deductions of lithological and hydrological conditions of the north-eastern sector of Akwa Ibom State, Southern Nigeria. *Res. J. Appl. Sci., Eng. Technol.*, 2011, **3**(8), 806–811.
9. Antonio Celso de Oliveira Braga, Walter, M. F. and Joao, C. D., Resistivity (DC) method applied to aquifer protection studies. *Rev. Bras. Geof.*, 2006, **24**(4), 573–581.
10. Henriet, J. P., Direct applications of the Dar-Zarrouk parameters in groundwater surveys. *Geophys. Prospect.*, 1975, **24**, 344–353.
11. Short, R. C. and Stauble, A. J., Outline geology of Niger Delta. *Am. Appl. Phys. Geol. Bull.*, 1967, **5**, 761–779.
12. George, N. J., Akpan, A. E., Obot, I. B. and Akpan Etuk, N. J., Geoelectrical investigation of erosion and flooding using the lithological composition of erosion and flood stricken roads in Ukanafun local government area of Akwa Ibom state. *Disaster Adv.*, 2008, **1**, 1–5.
13. Edet, A. E., Groundwater quality assessment in parts of eastern Niger Delta. *Environ. Geol.*, 1993, **22**, 41–46.
14. George, N. J., Akpan, A. O. and Umoh, A. A., Preliminary geophysical investigation to delineate the groundwater conductive zones in the coastal region of Akwa Ibom state, southern Nigeria, around the Gulf of Guinea. *Int. J. Geosci.*, 2013, **4**, 108–115; doi:10.4236/ijg.2013.4101.
15. Ibanga, J. I. and George, N. J., Estimating geohydraulic parameters, protective strength, and corrosivity of hydrogeological units: a case study of ALSCON, Ikot Abasisouthern Nigeria. *Arab. J. Geosci.*, 2016, **9**(5), 1–16.
16. George, N. J., Ibanga, J. I. and Ubom, A. I., Geoelectrohydrogeological indices of evidence of ingress of saline water into freshwater in parts of coastal aquifers of Ikot Abasi, southern Nigeria. *J. African Earth Sci.*, 2015, **109**, 37–46; http://dx.doi.org/10.1016/j.jafrearsci.2015.05.001.
17. George, N., Obianwu, V. and Udofia, K., Estimation of distribution of aquifer hydraulic parameters in the southern part of Akwa Ibom State, southern Nigeria using surficial geophysical measurements. *Int. Rev. Phys.*, 2011, **5**(2).
18. Obianwu, V., George, N. and Udofia, K., Estimation of hydraulic conductivity and effective porosity distribution using laboratory measurements on core samples in the Niger Delta, southern Nigeria. *Int. Rev. Phys.*, 2011, **5**(1), 1–12.
19. George, N. J., Ubom, A. I. and Ibanga, J. I., Integrated approach to investigate the effect of leachate on groundwater around the Ikot Ekpene Dumpsite in Akwa Ibom State, Southeastern Nigeria. *Int. J. Geophys.*, 2014, **2014**, 1–10; http://dx.doi.org/10.1155/2014/174589.
20. McNell, I. D., Electrical conductivity of soil rocks hydrol. *Process*, 2003, **17**, 1197–1211.
21. George, N. J., Atat, J. G., Umoren, E. B. and Etebong, I., Geophysical exploration to estimate the surface conductivity of residual argillaceous bands in the groundwater repositories of coastal sediments of EOLGA, Nigeria. *NRIAG J. Astron. Geophys.*, 2017, http://dx.doi.org/10.1016/j.nrjag.2017.02.001.
22. Zohdy, A. A. R., Eaton, G. P. and Mabey, D. R., Application of surface geophysics to groundwater investigations. *US Geol. Surv. Technol. Water Res. Invest.*, 1974, **D1**, 166.
23. Gemail, Kh. S., Ehistawy, A. M., El-Alfy, M., Ghoneim, M. F. and El-Bary, M. H., Abd; assessment of aquifer vulnerability to industrial waste water resistivity measurements. A case study along El-Gharbyia main drain, Nile Delta, Egypt. *J. Appl. Geophys.*, 2011, **75**, 140–150; doi:10.1016/j.jappgeo.2011.06.026.
24. van Stempvoort, D., Ewert, L. and Wassenaar, L., Aquifer vulnerability index: a GIS compatible methods for groundwater vulnerability mapping. *Can. Water Resour. J.*, 1992, **18**, 25–37.
25. Rottger, B., Kirsch, R., Scheer, W., Thomsen, S., Friborg, R. and Voss, W., Multi-frequency airborne EM surveys – a tool for aquifer vulnerability mapping. In *Near Surface Geophysics* (ed. Butler, D. K.), Tulsa, 2005, pp. 643–651.
26. Obianwu, I. V., Chimezie, C. I., Akpan, A. E. and George, N. J., Surficial geophysical deduction of the geomaterial and aquifer distribution at Ngor-Okpala Local Government Area of Imo State, southeastern Nigeria. *Cent. Eur. J. Geosci.*, 2011; doi:10.2478/s13533-011-0033-3.
27. WHO, Guidelines for drinking water quality incorporating the first addendum to third edition. Recommendations, vol. 1, Geneva; http://www.whoint/water_sanitation_helth/dwq/gdwg3rev/en/index.html, 2006.
28. Gogu, R. C., Hallet, V. and Dassargues, A., Comparison of aquifer vulnerability assessment techniques. Application to the Neblon river basin (Belgium). *Environ. Geol.*, 2003, **44**, 881–892.
29. George, N. J., Emah, J. B. and Ekong, U. N., Geohydrodynamic properties of hydrogeological units in parts of Niger Delta, southern Nigeria. *J. Afr. Earth Sci.*, 2015, **105**, 55–63.
30. Kalinski, R. J., Kelly, W. E., Bogardi, I. and Pesti, G., Electrical resistivity measurements to estimate travel through unsaturated groundwater protective layers. *J. Appl. Geophys.*, 1993, **30**, 161–173.
31. RIGW/IWACO, Development and management of groundwater resources in the Nile valley and delta project: assessment of groundwater pollution from domestic, agricultural and industrial activities. Internal project report, RIGW/IWACO, Cairo, 1990.

ACKNOWLEDGEMENTS. We are grateful to the water company that provided the geological and hydrochemical information used in this work. We are also grateful to the anonymous reviewers and the editor for improving the quality of paper through their thoughtful inputs.

Received 28 June 2016; revised accepted 4 March 2017

doi: 10.18520/cs/v113/i03/430-438